Remote Sensing of Environment 127 (2012) 341–356

Contents lists available at SciVerse ScienceDirect

Remote Sensing of Environment

journal homepage: www.elsevier.com/locate/rse

Observation uncertainty of satellite soil moisture products determined with physically-based modeling

Niko Wanders [a,*], Derek Karssenberg [a], Marc Bierkens [a,b], Robert Parinussa [c], Richard de Jeu [c], Jos van Dam [d], Steven de Jong [a]

[a] Department of Physical Geography, Faculty of Geosciences, Utrecht University, Utrecht, The Netherlands
[b] Deltares, Unit Soil and Groundwater Systems, Utrecht, The Netherlands
[c] Department of Hydrology and Geo-environmental Sciences, Faculty of Earth and Life Sciences, VU University Amsterdam, Amsterdam, The Netherlands
[d] Soil Physics, Ecohydrology and Groundwater Management Group, Wageningen University, Wageningen, The Netherlands

ARTICLE INFO

Article history:
Received 21 March 2012
Received in revised form 29 August 2012
Accepted 7 September 2012
Available online 13 October 2012

Keywords:
Soil moisture
Microwave remote sensing
Satellite uncertainty
ASCAT
AMSR-E
SMOS
SWAP-model

ABSTRACT

Accurate estimates of soil moisture as initial conditions to hydrological models are expected to greatly increase the accuracy of flood and drought predictions. As in-situ soil moisture observations are scarce, satellite-based estimates are a suitable alternative. The validation of remotely sensed soil moisture products is generally hampered by the difference in spatial support of in-situ observations and satellite footprints. Unsaturated zone modeling may serve as a valuable validation tool because it could bridge the gap of different spatial supports. A stochastic, distributed unsaturated zone model (SWAP) was used in which the spatial support was matched to these of the satellite soil moisture retrievals. A comparison between point observations and the SWAP model was performed to enhance understanding of the model and to assure that the SWAP model could be used with confidence for other locations in Spain. A timeseries analysis was performed to compare surface soil moisture from the SWAP model to surface soil moisture retrievals from three different microwave sensors, including AMSR-E, SMOS and ASCAT. Results suggest that temporal dynamics are best captured by AMSR-E and ASCAT resulting in an averaged correlation coefficient of 0.68 and 0.71, respectively. SMOS shows the capability of capturing the long-term trends, however on short timescales the soil moisture signal was not captured as well as by the other sensors, resulting in an averaged correlation coefficient of 0.42. Root mean square errors for the three sensors were found to be very similar ($\pm 0.05\,m^3m^{-3}$). The satellite uncertainty is spatially correlated and distinct spatial patterns are found over Spain.

1. Introduction

Soil moisture is an important variable in many applications and environmental studies, such as numerical weather prediction (Drusch, 2007), global change modeling (Henderson-Sellers, 1996), predicting surface runoff (Brocca et al., 2010), drought monitoring (Sheffield & Wood, 2007) and modeling evaporation (Miralles, Holmes, et al., 2010). In small catchments (700 km^2) soil moisture assimilation has been shown to improve discharge simulation (Brocca et al., 2010); the impact in larger scale river basins remains unknown. At this large scale, ground based soil moisture measurements are relatively scarce and therefore lack sufficient spatial density to be accurately up-scaled to improve flood forecasting for large river basins. Soil moisture is highly variable in space and time and thus a high spatial and temporal resolution of observations is required to retrieve good estimates of the actual soil moisture content (Western et al., 2002).

A possible solution to obtain spatially averaged soil moisture for large river basins is the use of soil moisture retrievals from spaceborn sensors measuring in the microwave frequencies. For several years passive and active microwave observations have been used for the retrieval of soil moisture from the Earth's surface. The current Soil Moisture and Ocean Salinity (SMOS) mission observes the Earth's surface in the L-band (1.41 GHz) frequency (Wigneron et al., 1995), because such low frequency observations are most sensitive to soil moisture. SMOS is the first dedicated satellite observing soil moisture from space and was launched in November 2009. In the past, several passive microwave sensors, such as the Advanced Microwave Scanning Radiometer-EOS (AMSR-E), have been used to retrieve soil moisture using multi-channel observations obtained at higher microwave frequencies (e.g. Njoku et al., 2003; Owe et al., 2008). AMSR-E, onboard NASA's Aqua satellite was launched in 2002 and was recently (October 2011) switched off due to rotation problems with its antenna. Also, several active microwave sensors, such as the Advanced Scatterometer (ASCAT) onboard ESA's MetOp satellite, were used for the same purpose. Backscatter measurements at three different azimuth angles are converted to surface soil moisture (Naeimi et al., 2009). Microwave

* Corresponding author. Tel.: +31 30 253 2988.
E-mail address: n.wanders@uu.nl (N. Wanders).

0034-4257/$ – see front matter © 2012 Elsevier Inc. All rights reserved.
http://dx.doi.org/10.1016/j.rse.2012.09.004

observations are largely unaffected by solar illumination and cloud cover, but can be influenced by topography and active precipitation. Additionally, several studies (De Jeu et al., 2008; Dorigo et al., 2010; Parinussa et al., 2011) showed a decreasing quality of soil moisture retrievals with increasing vegetation density.

Microwave remote sensing provides areal (625–2500 km^2) averaged soil moisture content with a high temporal resolution (revisit time 1–3 days), which could be used for large scale hydrological applications (Walker & Houser, 2004). However, in operational hydrological modeling (e.g. data assimilation schemes) it is important to provide a good estimate of the uncertainty of the remotely sensed soil moisture product (Crow & Ryu, 2009). Some studies successfully used remotely sensed soil moisture in assimilation schemes showing the potential use of them to improve discharge simulations (e.g. Brocca et al., 2010; Draper et al., 2011). These studies used a single satellite product and made often arbitrary assumptions on the uncertainties in retrieved soil moisture. Also, spatio-temporal variation in uncertainty is mostly neglected. However, to make optimal use of (multiple) remotely sensed soil moisture products in assimilation schemes, it is essential to determine the magnitude and spatial structure of the uncertainties of each product (Van Leeuwen, 2009).

One approach to determine the uncertainty of satellite soil moisture products is to use ground based observations. Unfortunately, this approach is generally hampered by a lack of ground based observation networks with sufficient spatial density (low coverage) to allow for accurate upscaling to the resolution of satellite based soil moisture retrievals (Scipal et al., 2008). Recently, in-situ observations became more readily available (Dorigo et al., 2011) resulting in several studies (e.g. Miralles, Crow & Cosh, 2010) providing meaningful information about the differences in spatial resolution between in situ and remotely sensed soil moisture products. Evaluation results from these more traditional in situ validation were performed by e.g. Walker and Houser (2004), Wagner et al. (2007), Albergel et al. (2012). However, these studies did not take into account the difference in spatial resolution of in-situ observations and remotely sensed soil moisture. In these studies, it is assumed that the in-situ observation provides a valid value for the footprint scale modeled soil moisture while this assumption might not always be valid (Crow et al., 2012). Additionally, there is only a small number of in-situ soil moisture networks available with enough coverage to accurately up-scale in-situ observations to the spatial resolution of microwave products. For this reason several evaluation techniques (Crow & Zhan, 2007; Crow et al., 2010; Dorigo et al., 2010; Scipal et al., 2008) have been proposed which circumvent the need for extensive ground-based soil moisture observations.

An additional approach to validate remotely sensed soil moisture is process-based unsaturated zone modeling. An advantage of a physically-based unsaturated zone models is their capability to represent spatio-temporal variation in meteorological forcing, soil parameters and unsaturated zone processes (De Lannoy et al., 2006; Finke et al., 1996). This enables a validation at the spatial resolution of the microwave soil moisture products (625–2500 km^2). Matching the spatial scales of remotely sensed soil moisture products and unsaturated zone models is essential to enable the calculations of the uncertainty of the remote sensing product itself (Bierkens et al., 2000). In this study, the physically based Soil Water Atmosphere Plant model (SWAP, Van Dam (2000) Kroes et al. (2008)) was applied, which was successfully used in various studies (e.g. Baroni et al., 2010; Singh et al., 2006). The SWAP model integrates local information (e.g. meteorological stations, soil data) with high spatial resolution (km-scale) remotely sensed imagery (e.g., Leaf Area Index). Combining information from these different sources allows for up-scaling (also referred to as aggregating) of the high spatial resolution unsaturated zone model to match the spatial resolution of the remotely sensed soil moisture product. The SWAP model uses a high-resolution multi-layer approach in the vertical to deal with the different observation characteristics of the different satellite products, resulting in simulated soil moisture content at several depths, including the top-layer.

The assessment of uncertainty in modeled soil moisture is mostly unknown because uncertainties are not known at the satellite scale and errors made by the hydrological model are ascribed as satellite error. In reality the model uncertainty could be very large and satellite uncertainty is highly overestimated, because model calibration is often done at locations with a single measurement per model grid point of 64–2500 km^2. In previous studies the assessment of uncertainty in modeled soil moisture was most of the time unknown because the magnitude and spatial structure of the error are not known. To deal with this problem, model uncertainties and uncertainties of the input parameters are considered in this study when up-scaling the SWAP model to satellite footprint scale.

The aim of this study is to accurately up-scale the high-resolution unsaturated zone model in order to provide a detailed assessment of the uncertainty of the satellite derived soil moisture product at the correct spatial and temporal support. To achieve this aim, the performance of the SWAP model was evaluated at different spatial scales and finally up-scaled to match the coarse resolution satellite soil moisture products. To deal with the unique observation depths of the different microwave systems a high-resolution multi-layer model simulation of SWAP was used. The SWAP model was validated for the REMEDHUS soil moisture network in Spain to investigate if the model could be applied in other regions of Spain for satellite validation, assuming the model could be used without further modifications. Thereafter, soil moisture was modeled for 79 locations in Spain and compared to timeseries of remotely sensed soil moisture product (AMSR-E, SMOS and ASCAT) and the magnitude and spatial structure of the uncertainties was determined.

2. Material and methods

2.1. Satellite data

Three satellites that measure soil moisture are used for this intercomparison study, namely SMOS, ASCAT and AMSR-E (Table 1). The SMOS satellite was launched on 2 November 2009 and the data for the level 2A soil moisture product have been available since January 2010 (Kerr et al., 2010). SMOS is the first dedicated soil moisture satellite and uses fully polarized passive microwave signals at 1.41 GHz (L-band) observed at multiple angles. SMOS is developed to measure soil moisture content with a target accuracy (standard error) of 0.04 m^3 m^{-3} (Kerr et al., 2001). The overpass time at the equator is 6:00 AM/PM, with a maximum revisit time of 3 days at equatorial latitudes. In this study only morning overpasses have been used, because between midnight and early morning, the soil moisture has an equilibrium state and is not influenced by bare-soil evapotranspiration. The spatial resolution of SMOS is 35–50 km depending on the incident angle and the deviation from the satellite ground track. The innovative observation technique and algorithms of SMOS are still relatively new and the retrieval algorithm is under constant development. Radio frequency interference (RFI) at L-band have been reported over large parts of Europe and Asia, which may impact its

Table 1
General sensor properties relevant for this study.

	SMOS	ASCAT	AMSR-E
Frequency (GHz)	1.41	5.3	6.9
Microwave type	Passive	Active	Passive
Spatial resolution (km)	35–50	25	36–54
Max revisit time (days)	3	3	3
Observation depth (cm)	0–5	0–2	0–2
Descending overpass (h)	6:00 PM	9:30 AM	1:30 AM

soil moisture retrieval (Anterrieu, 2011). RFI will affects SMOS soil moisture retrievals and especially for Europe the observations in the first half of 2010 are partly contaminated by RFI. In this study we have removed these RFI influenced observations by filtering the data. SMOS retrievals with an RFI flag raised have been removed from the analysis as were retrievals with a large retrieval uncertainty (DQX $\geq 0.04\ m^3 m^{-3}$) uncertainty. SMOS data are obtained from the ESA and reprocessed data (Level 2 processor v501) from 2012 have been used for the entire evaluation period. For more detailed information about the SMOS algorithm and the level 2 product the reader is referred to Kerr et al. (2012).

AMSR-E is a multi-frequency (6 bands from 6.9 to 89.0 GHz) passive microwave radiometer and was the first widely used sensor for soil moisture retrievals. AMSR-E is in a sun synchronized orbit with local equator overpass times at 01:30 AM/PM. Several algorithms estimating surface soil moisture from AMSR-E observations exist (e.g. Njoku et al., 2003; Owe et al., 2008). All these algorithms use a combination of observations in several frequencies and/or polarizations, and some use auxiliary data. One of the algorithms using exclusively satellite observations is the Land Parameter Retrieval Model (LPRM) developed by scientist at NASA and the VU Amsterdam (VUA). This model uses a simple radiative transfer equation to retrieve soil moisture and vegetation optical depth from horizontal and vertical polarized brightness temperatures by partitioning the observed signal into its respective soil and vegetation emission components (e.g. De Jeu & Owe, 2003; Meesters et al., 2005). LPRM soil moisture products have been extensively validated against in situ observations (e.g. De Jeu et al., 2008; Draper et al., 2009; Wagner et al., 2007), models (e.g. Bisselink et al., 2011; Crow et al., 2010; Loew et al., 2009) and other satellite products (Dorigo et al., 2010; Wagner et al., 2007). These studies show that LPRM soil moisture captures a large part of the temporal variability (as shown by the correlation coefficient), which was confirmed by Crow et al. (2010) using a completely different approach and using soil moisture anomalies rather than absolute values. This skill was the main driver to select LPRM soil moisture retrievals for this study. AMSR-E makes both day- and night-time observations. In existing studies only night-time observations were used as it was shown that soil moisture retrievals based on these are more reliable than those based on day-time observations (De Jeu et al., 2008).

Unlike SMOS and AMSR-E, ASCAT uses active microwave at a frequency of 5.3 GHz (C-band) to determine the soil moisture content (Naeimi et al., 2009; Wagner et al., 1999). ASCAT uses a change detection method in which the changes in the amount of backscatter are linearly related to changes in soil moisture content and vegetation cover (Naeimi et al., 2009). Data is provided as relative soil moisture content, with respect to the wettest and driest soil moisture conditions measured during the lifetime of ASCAT (Wagner et al., 1999). The spatial resolution of ASCAT is around 25 km and the temporal resolution equals a revisit time of 3 days at 9:30 AM/PM around equatorial latitudes. Only descending passes of ASCAT (9:30 AM) have been used. Reprocessed ASCAT data were obtained from the TU Wien archive.

All satellite soil moisture level 2 products are evaluated on an equal area Discrete Global Grid product (DGG). For the SMOS and ASCAT soil moisture product a DGG is available (Bartalis, Kidd & Scipal, 2006), while for the AMSR-E product this DGG is not available. Therefore, the AMSR-E data were projected on the DGG of SMOS using the nearest neighbor approach because both satellites have roughly the same spatial resolution. The DGG of ASCAT uses equally spaced areas of 12.5 km while the other DGG uses a slightly lower resolution of 15 km between points.

ASCAT data, which are by default expressed as values between 0 and 100 (−) indicating, very dry and very wet conditions, respectively, was converted to the dynamic range of the model. Although the passive microwave satellite missions, SMOS and AMSR-E, give absolute soil moisture values in $m^3\ m^{-3}$, all satellite data was converted using the same approach, to enable a comparison of the absolute errors of satellites. The new satellite values $\theta_{s,new}$ in $m^3\ m^{-3}$ used here are calculated by:

$$\theta_{s,new} = \frac{\theta_s - \theta_{s,5}}{\theta_{s,95} - \theta_{s,5}} \left(\theta_{m,95} - \theta_{m,5}\right) + \theta_{m,5} \quad (1)$$

where θ_s are the observed satellite soil moisture values ($m^3\ m^{-3}$ or −), θ_{95} and θ_5 are the *95th* and *5th* percentiles of satellite soil moisture values per DGG location respectively ($m^3\ m^{-3}$ or −), $\theta_{m,95}$ and $\theta_{m,5}$ are the 95th and 5th percentiles of modeled soil moisture values for the same DGG location ($m^3\ m^{-3}$ or −). Unlike cumulative density function (CDF) matching (e.g. Brocca et al., 2011; Liu et al., 2010) this approach has the advantage that the shape of the probability density function of each product remains the same and temporal dynamics as well as temporal statistics like correlation are not influenced.

For the retrieval of near surface soil moisture frozen soils and Radio Frequency Interference (RFI) hamper soil moisture observations. Frozen soils hamper the soil moisture retrieval due to changes in the dielectric constant when water freezes. Therefore, retrievals done with an air temperature below 4 °C were excluded from the analysis. For AMSR-E these observations are excluded by the LRPM algorithm because AMSR-E is capable of measuring the soil surface temperature. RFI distort the incoming signal and the microwave signals measured by the satellites. Although the retrievals of all satellites suffer from RFI presence, SMOS appears to have the most RFI-related problems (Kerr & Pla, 2011). From the second part of 2010 the influence of RFI has however significantly been reduced for most countries in Europe, including Spain.

2.2. In-situ soil moisture measurement and meteorological data

The validation of the three remotely sensed near surface soil moisture products was carried out for the mainland of Spain. Spain was selected because of the presence of the REMEDHUS soil moisture network providing data for the period 2006–2011 at a high temporal resolution for a relatively large number of sampling locations (Martínez-Fernández & Ceballos, 2003; Sánchez et al., 2010). From the International Soil Moisture Network (Dorigo et al., 2011), in-situ soil moisture content is available at a depth of 5 cm for 22 locations (Fig. 1). An additional advantage of Spain is the availability of a high number of meteorological stations distributed throughout Spain.

Data from 79 meteorological sites in Spain (Fig. 2) obtained from the Spanish meteorological service (AEMET), were used for the

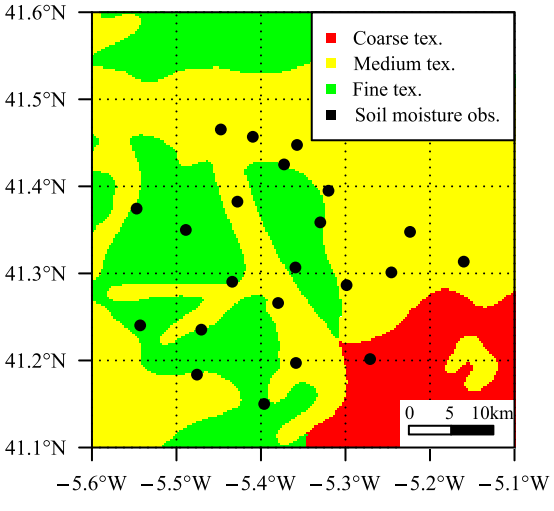

Fig. 1. Locations of 22 soil moisture observation points and soil texture information derived from the JRC European soil texture map (Van Liedekerke et al., 2006) for the REMEDHUS site in Spain.

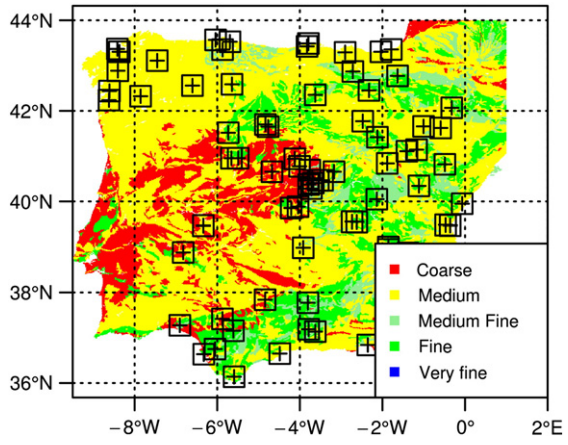

Fig. 2. Soil map of Spain overlaying with meteorological sites (crosses) and model areas used for comparison with satellite soil moisture (squares), open water is excluded from the simulation.

evaluation of the three remotely sensed soil moisture products. These meteorological sites have meteorological data for the period January 2009–July 2011 including precipitation and the variables required to estimate Penman–Monteith reference evapotranspiration. It is also assumed that up to a maximum distance of 35 km ground observations provide a good estimate of the precipitation and evapotranspiration for soil moisture modeling. The interception was calculated with the 8-days composite of the Leaf Area Index (LAI) from the MODIS sensor, provided at 1×1 km spatial resolution (Myneni et al., 2003). To determine Van Genuchten soil parameters for each simulation the JRC European soil texture map with a resolution of $1\times1\,km$ was used (Van Liedekerke et al., 2006). Joint probability distributions of the Van Genuchten soil physical parameters (Van Genuchten, 1980) per soil texture class were obtained from Meyer et al. (1997). With these joint distributions, spatial variability within each soil texture class is introduced such that the correlation between Van Genuchten parameters is preserved.

2.3. SWAP model set-up

The Soil-Water-Atmosphere-Plant model (SWAP) is a physically-based model simulating flow processes in the unsaturated zone (Kroes et al., 2008; Van Dam, 2000). A short overview of the most important concepts and assumptions is given below. Soil water flow in the SWAP model is calculated with the Richards equation (Richards, 1931):

$$\frac{\partial\theta}{\partial t}=\frac{\partial}{\partial z}\left[K(\theta)\left(\frac{\partial h}{\partial z}\right)+1\right]-S \tag{2}$$

where θ is volumetric soil moisture content ($m^3\ m^{-3}$), h matrix head (m), z the elevation (m, positive upwards), t time (d), S a sink of the system (md^{-1}) which accounts for external losses like transpiration and evaporation and $K(\theta)$ the conductivity (md^{-1}) as a function of water content (θ). The SWAP model uses an implicit, backward, finite difference scheme to solve the Richards equation. The Mualem–Van Genuchten relations are used to determine the hydraulic properties of the soil. The soil water content, θ, ($m^3\ m^{-3}$) is modeled by:

$$\theta(h)=\theta_r+\frac{(\theta_s-\theta_r)}{\left[1+|\alpha h|^n\right]^{1-1/n}} \tag{3}$$

where, h is the pressure head (m), θ_r, θ_s are the residual and saturated soil moisture content ($m^3\ m^{-3}$), respectively, and α (−) and n (−) are the shape parameters (Van Genuchten, 1980). The parameters of Eq. (3) are derived from the soil texture map. The model runs with an hourly timestep and is composed of 28 vertical layers representing the soil up to a depth of 150 cm below the soil surface (Fig. 3). The first 10 cm was simulated using 10 layers of 1 cm, followed by 8 layers of 5 cm, followed by 10 layers of 10 cm. This high vertical resolution of soil layers was used in order to have a detailed estimate of the soil moisture content at different penetration depths of the radar signal. A free drainage bottom boundary condition is applied to the model. Soil water uptake by roots is assumed to be evenly distributed up to a depth of 70 cm, to simulate and average vegetation. Daily potential evapotranspiration was calculated with the Penman–Monteith equation following Allen et al. (2006) which requires air pressure, wind speed, air humidity and daily temperature (maximum, mean, minimum) from meteorological stations. The potential fluxes of transpiration and evaporation are modeled as a function of the LAI. The actual transpiration flux is calculated as described by Feddes et al. (1988). The actual evaporation flux is the minimum of the potential evaporation, the maximum soil water flux and the maximum evaporation flux according to Black et al. (1969). Interception of precipitation was calculated following Von Hoyningen-Hüne (1983) with an maximum interception capacity of 0.25 mm LAI^{-1}.

In this study a model was used which is normally applied to field scale unsaturated zone modeling instead of large scale applications. Lateral flow might be very important on the field scale (Harter & Hopmans, 2004), but is negligible at the support of satellites and is thus assumed zero. The effect of irrigation in Spain is assumed to be small since throughout Spain less than 10% of the land is irrigated (Siebert et al., 2007).

2.4. Evaluation of model performance and sensitivity analysis

The uncertainty of modeled soil moisture is assessed, using a Monte Carlo approach by perturbing the following input data and

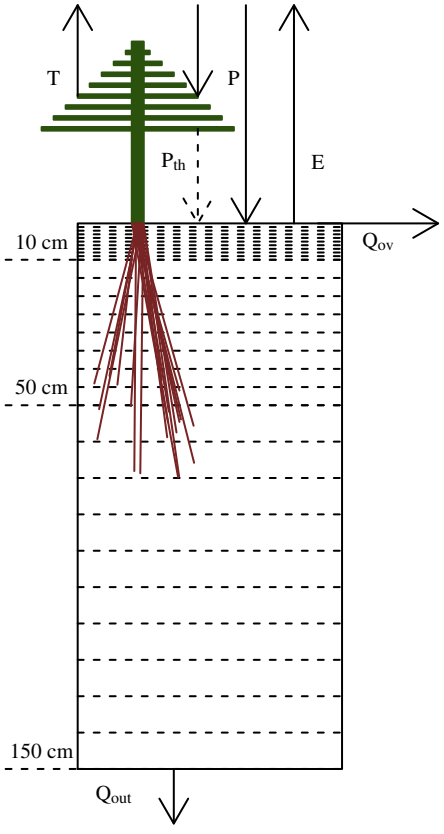

Fig. 3. SWAP model set-up, precipitation (P), evaporation (E), through fall from vegetation (P_{th}), transpiration from leaves (E_i), overland flow (Q_{ov}) and bottom out flux (Q_{out}). Model layers are indicated by the dotted horizontal lines.

parameters of SWAP: precipitation (P), evapotranspiration (E), LAI and soil properties. Since P, E, LAI and soil physical parameters are found to have the largest influence on the simulation of near surface soil moisture (De Lannoy et al., 2006; Finke et al., 1996) other parameters were kept constant and are assumed to have a negligible effect on the uncertainty of modeled soil moisture. The structural error was also not taken into account since is was assumed to be subordinate to errors in the model forcing and parameters.

Three error models were used to add uncertainty to the input data and parameters of the SWAP model (Table 2). In the Continuous Spatial Uncertainty Model (CSUM), variogram models and observations were used to create realizations of meteorological variables conditioned to observed values at the meteorological stations, $P_{obs}(x,t)$. For precipitation ($P(x,t)$,mm) it is assumed that:

$$P(x,t) = Z(x,t)^2 \tag{4}$$

where $Z(x,t)$ is a Gaussian distribution variable with spatial index x (Schuurmans et al., 2007). The spatial correlation of $Z(x,t)$ ($mm^{0.5}$) is given by a linear variogram:

$$\gamma(h) = (s-n)\frac{h}{r} + n \tag{5}$$

where $\gamma(h)$ is the variance as a function of the lag h (m), the sill s (mm), the nugget n (mm), and the range r (m), of the variogram. The variogram was computed with observations from all 79 stations over a period of 2.5 years without making any distinction between the different seasons or different spatial scale of the precipitation events. Since the required data to create variogram models for individual precipitation events is not available it was decided to use a single variogram model. With this variogram a Gaussian random simulation conditioned to the observations $p_{obs}(t)$(mm), was performed, obtaining realizations of maps of precipitation, $P(t)$(mm), for each day of the simulation. Following the same approach a variogram model was fitted to the Penman–Monteith reference evapotranspiration calculated at the station locations. Evapotranspiration was not transformed and was assumed to have a Gaussian distribution with a linear variogram (Eq. 5). This model was used to simulate possible fields of evapotranspiration for the reference locations, in order to assess the effects of evapotranspiration uncertainty.

The Continuous Local Uncertainty Model (CLUM) is used to introduce uncertainty in LAI values and is given by:

$$\mathrm{LAI}_n(t) = \mathrm{LAI}_o(t)\cdot X(\mu,\sigma) \tag{6}$$

where LAI_n is a random variable ($m^2\ m^{-2}$), LAI_o is the observed MODIS LAI value ($m^2\ m^{-2}$), $X(\mu,\sigma)$ is a Gaussian random variable with mean, μ, and standard deviation, σ. In this study μ (−) is set to 1 and σ (−) was based on a study from (Yang et al., 2006) and is set to 0.1 introducing random error in the LAI used for the calculations of the SWAP model.

Table 2
Description of variables and used uncertainty model for each perturbed parameter of the SWAP model. Error models given are the Discrete Local Uncertainty Model (DLUM), Continuous Spatial Uncertainty Model (CSUM) and Continuous Local Uncertainty Model (CLUM).

Var	Description	Source	Error model
θ_s	Saturated soil moisture	(Meyer et al., 1997)	DLUM
θ_r	Residual soil moisture	(Meyer et al., 1997)	DLUM
$K(\theta)$	Unsaturated conductivity	(Meyer et al., 1997)	DLUM
n	Van Genuchten n-parameter	(Meyer et al., 1997)	DLUM
α	Van Genuchten α-parameter	(Meyer et al., 1997)	DLUM
P	Precipitation	Meteo station	CSUM
E	Evapotranspiration	Meteo station	CSUM
LAI	Leaf Area Index	MODIS satellite	CLUM

The Discrete Local Uncertainty Model (DLUM) is applied for the soil physical parameters and uses local properties to add uncertainty to parameters. With the DLUM the soil texture of a location is conditionally changed for 20% of the locations. Since errors in soil texture maps are not uncommon (Hengl & Toomanian, 2006) this 20% error was introduced to account for the effect of misclassification. Realizations of soil texture were created by randomly changing the soil texture of cells. In creating a realization, for each cell, the probability of a newly selected soil class (c) is calculated as:

$$Pr(c) = \frac{n_{c,i}}{N - n_{c,j}} \tag{7}$$

where $n_{c,i}$ and $n_{c,j}$ are the relative occurrences of the perturbed and observed soil texture over Spain respectively and N is the total number of pixels on the 1×1 km soil texture map. If a misclassification occurs, the soil texture is changed and will not be ascribed to j again resulting in newly assigned texture classes.

The predictive QQ-plot as described by Laio and Tamea (2007) was used to determine if the model uncertainties and combined uncertainty of the input data could explain the variation between different points of the REMEDHUS network. The predictive QQ-plot is a measure to check whether the obtained Monte Carlo simulation results in a probability density function (PDF) that corresponds to the PDF of the model prediction errors. In the predictive QQ-plot the probability integral transforms to:

$$z_i = \int_{-\infty}^{x} f(x_i)\mathrm{d}x \tag{8}$$

where $f(x_i)$ is the PDF of model outputs obtained from the uncertainty analysis (Monte Carlo simulation), x_i is the value at observation location i and z_i the associated cumulative probability. Thus, z_i gives the probability of the observed values with respect to the distribution of predicted values from the Monte Carlo simulation. The z_i values are plotted against their cumulative density function, $Rank_i(x_i)$, which is produced from the observation rank rank(x_i):

$$\mathrm{Rank}_i(x_i) = \frac{\mathrm{rank}(x_i)}{n+1} \tag{9}$$

where n is the total number of x_i values. When the z_i plotted against the Rank_i are on the 1:1 line, the PDF from the uncertainty analysis correctly represents the prediction errors and the predictions are unbiased. The non-parametric Kolmogorov–Smirnov test is used to evaluate whether the results are within the 95% confidence interval of the 1:1 line. More details of the predictive QQ-plot are given in Laio and Tamea (2007).

The performance of the SWAP model at the REMEDHUS site was evaluated using the Pearson correlation (R, Eq. A.1), Root Mean Square Error (RMSE, Eq. A.2) and model bias, bias_m(m^3m^{-3}):

$$\mathrm{bias}_m = \mu_o - \mu_m \tag{10}$$

where μ_o and μ_m respectively are the average observed and modeled soil moisture over the entire simulation period ($m^3\ m^{-3)}$ where a negative value indicates an underestimation of the soil moisture. The REMEDHUS site was not used for calibration of the model, only to evaluate the model and to determine the errors in the modeled soil moisture and input data. Soil moisture was simulated for the entire period from 2006 to 2010. In total 2000 simulations were done with perturbed parameters and input data for the REMEDHUS site in order to accurately capture the full probability density functions of all parameters and input data. This high number of simulations also allowed to accurately calculate the model uncertainty and study the model sensitivity to the full range of possible parameters sets.

For all selected 79 meteorological stations, a Monte Carlo approach (150 realizations) was used to determine the overall modeled

uncertainty at satellite footprint scale. Soil moisture around the meteorological site was simulated for a 0.5°×0.5° area centered around the location of the meteorological station. Larger simulation areas would require the use of interpolation techniques to derive values between stations which could result in large uncertainties leading to high model uncertainties. The comparison between SWAP and different satellite products was made on the scale of the specific satellite DGG by upscaling SWAP to the DGG resolution ($\approx 150-225\ km^2$) by taking the arithmetic mean of the model simulations over the satellite footprint area and penetration depth. The comparison between the model and different satellites is done at the overpass time of the satellite with a maximum temporal mismatch of 30 minutes due to the one hour simulation time steps. The correlation, random error and biases between satellite and the mean of the Monte-Carlo simulations were used as performance indicator of the satellite soil moisture for each location. The correlation R for the evaluation of the remotely sensed soil moisture is calculated using Eq. (A.3).

The satellite soil moisture is considered as a random variable composed of three terms:

$$\Theta_s(t) = \Theta_r(t) + \varepsilon_s - \text{bias}_s \tag{11}$$

where $\Theta_s(t)$ is a random variable ($m^3\ m^{-3}$) representing the satellite soil moisture, $\Theta_r(t)$ is the real soil moisture ($m^3\ m^{-3}$), ε_s is the random error of satellite soil moisture ($m^3\ m^{-3}$) and bias_s is the systematic error of the satellite soil moisture ($m^3\ m^{-3}$). The satellite soil moisture bias (bias_s) compared to the model is calculated by:

$$\text{bias}_s = \mu_s - \mu_m \tag{12}$$

where μ_s is the average satellite soil moisture over the entire simulation period ($m^3\ m^{-3}$). In this study it is assumed that the bias_s remains constant over time. The modeled soil moisture is considered as a random variable given by:

$$\Theta_m(t) = \Theta_r(t) + \varepsilon_m \tag{13}$$

where $\Theta_m(t)$ is a random variable ($m^3\ m^{-3}$) representing the modeled soil moisture and ε_m is the random error of modeled soil moisture ($m^3\ m^{-3}$). The satellite error over time is computed with:

$$\epsilon_s(t) = \theta_s(t) - \theta_m(t) - \epsilon_m(t) - \text{bias}_s \tag{14}$$

where $\epsilon_s(t)$ is the satellite error as a function of time ($m^3\ m^{-3}$) and $\epsilon_m(t)$ is the model error over time ($m^3\ m^{-3}$), where it is assumed that $\epsilon_m(t) = \theta_r(t) - \theta_m(t)$. In addition the satellite standard error is calculated as:

$$\hat{\sigma}\epsilon_s = \sqrt{\frac{\sum_{t=1}^{N}(\theta_s(t) - \theta_m(t) - \text{bias}_s)^2}{N}} - \hat{\sigma}\epsilon_m \tag{15}$$

where $\hat{\sigma}\epsilon_s$ is the standard deviation of the random satellite error (ε_s) over the time period 1…N and $\hat{\sigma}\epsilon_m$ is the standard deviation of ε_m (obtained from the Monte Carlo analysis). It is assumed that there is no correlation between the errors of the model and satellite and therefore the covariance is omitted in Eq. (15).

The calculated $\hat{\sigma}\epsilon_s$ (Eq. 15) values for each location related to geographical and climatological properties of all 79 meteorological stations, in order to create a better understanding of the satellite performance as function of these environmental variables and possible error sources. Previous studies stated that several external factors may have a negative influence on soil moisture mapping performance, namely topography (Engman & Chauhan, 1995), dense vegetation (De Jeu et al., 2008; Njoku & Li, 1999; Parinussa et al., 2011), soil moisture wetness conditions (Troch et al., 1996) and land-sea contamination (Njoku & Kong, 1977; Owe et al., 2008). The effect of these external factors on the mapping performance of microwave satellites was tested using the SWAP model simulations over Spain. External factors evaluated include the gradient (*Grad*), calculated as the average slope (%) over the support of the satellite, distance to the sea (*Sea*) calculated as the shortest distance between the location and the coast (*km*). To calculate these values the Digital Elevation Model of Spain, acquired by the Shuttle Radar Topography Mission, was used on a 30 meter resolution. The average soil moisture content (μ_m,m^3m^{-3}) and standard deviation of soil moisture content (σ_m,m^3m^{-3}) over time were calculated per location. Additionally the impact of the Leaf Area Index (LAI(t),m^2m^{-2}) and the time dependent soil moisture content ($\theta(t)$,m^3m^{-3}) on the satellite error was evaluated. Their influence is evaluated on the time dependent satellite error $\epsilon_s(t)$, where (t) indicates the variation of error over time.

The spatial pattern of correlation (R) and standard error ($\hat{\sigma}\epsilon_s$) over Spain were studied for the three satellite products. Additionally, the spatial correlation between errors ($\epsilon_s(t)$) was investigated in order to determine if errors are randomly distributed or correlated in both space and also time. A variogram was calculated to determine to what distance errors are correlated (Cressie, 1993), changes in these patterns through seasons are not taken into account.

3. Results

3.1. SWAP model validation with in-situ observations

The obtained semi-variogram models of the square root of precipitation and Penman–Monteith reference evaporation from the meteorological observations are shown in Fig. 4. The precipitation semi-variogram models obtained in this study show a great resemblance with those calculated for medium and large extent precipitation events (Schuurmans et al., 2007). It is assumed that these variogram models are valid to produce a realistic simulation of precipitation and reference evaporation uncertainty over Spain.

Modeled soil moisture at 5 cm depth was validated against in-situ measurements to examine if the SWAP model is capable of producing correct near-surface soil moisture simulations. Results show that mean modeled soil moisture by SWAP is in good agreement with the mean observed soil moisture values of the REMEDHUS network 2010 (Fig. 5). A high correlation ($R = 0.878$) is found between the SWAP model mean and mean of observations, while the root mean square error (RMSE) is low (0.025 $m^3\ m^{-3}$). A small positive bias_m of 0.01 $m^3\ m^{-3}$ (Eq. 10) exists between model mean and the observations which is mainly caused by overestimated soil moisture values in May and June. This behavior is probably caused by an underestimation of evapotranspiration and only seen at the REMEDHUS site in

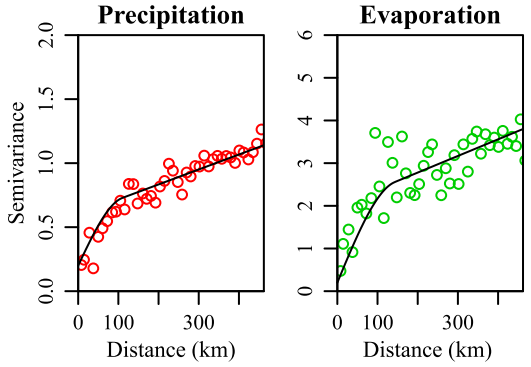

Fig. 4. Semi-variograms of the square root of observed precipitation ($mm^{0.5}$) and Penman–Monteith reference evaporation (mm) for the period January 2009–June 2011 over Spain based on observations of 79 meteorological stations.

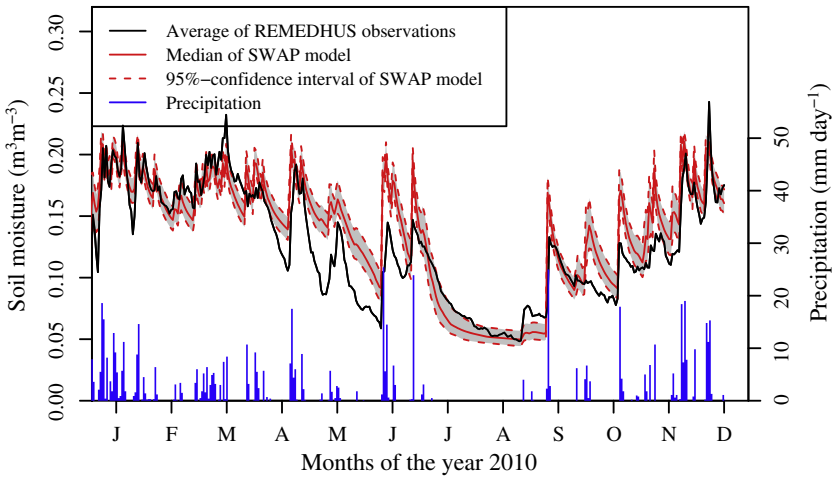

Fig. 5. Comparison between the average SWAP modeled soil moisture at the REMEDHUS network and the average of the in-situ observations of the REMEDHUS network for the year 2010.

2010. It was not found in other years. From the results of the REMEDHUS site it was found that the Van Genuchten pore-size distribution parameter (n,−) should not exceed 2.55, which indicates very coarse sand. Higher values (e.g. coarse gravel) could lead to unrealistic soil moisture simulations at REMEDHUS and in some situations could lead to model instability. The model was also evaluated by comparing the full probability density functions (PDF) of the model and the 22 observations at the REMEDHUS network with the predictive QQ-plot (Eqs. (8) and (9)). The predictive QQ-plot (Fig. 6) shows that the modeled soil moisture is within the 95%-confidence interval of the Kolmogorov–Smirnov test (KS-test). The bias_m of 0.01 $m^3\ m^{-3}$ calculated with Eq. (10) was also found in the predictive QQ-plot. The SWAP model slightly overestimates the amount of low soil moisture values compared to the observations as seen from a small deviation below 0.2 $m^3\ m^{-3}$ soil moisture content. This deviation is however not significant as shown by the KS-test.

From Figs. 5 and 6, as well as from the high R, low *RMSE* and low bias, it is concluded that the overall performance of the SWAP model as well as the estimated uncertainty of the input data and parameters is of good quality for a proper simulation of observed soil moisture at 5 cm depth. The predictive QQ-plot shows that variation within and between soil units is well captured by the model at the REMEDHUS network. Without taking into account the structural error of the SWAP model, the simulations of soil moisture show a good agreement with the observations at a the scale of the satellite footprint (Fig. 5) as well as with local observations points of the REMEDHUS network (Fig. 6). Given the obtained results the SWAP model is used with confidence in other areas in Spain.

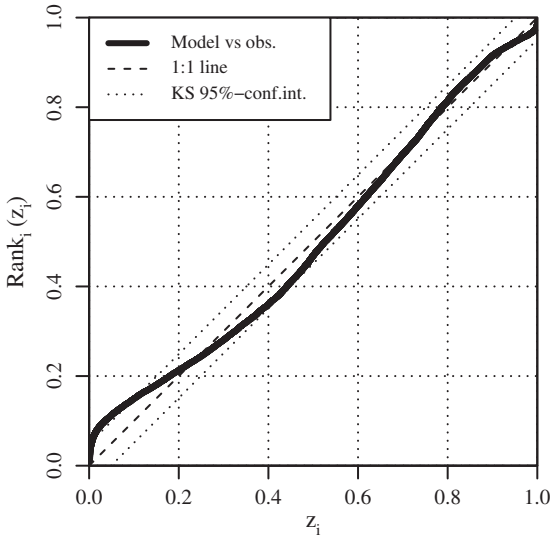

Fig. 6. Predictive QQ-plot for validation of the observations of the REMEDHUS network (Eq. 8) against the SWAP model (Eq. 9) for the period 2006–2010. The 95% confidence interval of the Kolmogorov–Smirnov (KS) test is indicated as well as the 1:1 line.

3.2. Remotely sensed soil moisture inter-comparison over Spain

The locations of the 79 reference stations, including the area modeled around each station (up to 35 km) were used as reference locations in this study (Fig. 2). At each reference location, a different number of satellite retrievals is available depending on the resolution of the Digital Global Grid (DGG) and the positioning of the reference location on the DGG of each satellite (Table 3). In general, the number of ASCAT DGG points per reference location is higher due to the higher density of the DGG (≈12.5 to 15 km). As an example, Fig. 7 presents time series of soil moisture retrievals from the different satellites in Northwest Spain (42.9 °N, 2.7 °W). Note that the values of $\theta_m(t)$ differ between satellites due to the different spatial resolutions of the data in both vertical and horizontal scales (see Table 1). More example time series for all satellites are given in Appendix B.

For AMSR-E the trend of high soil moisture values in winter and low soil moisture values in summer is captured very well resulting in low satellite errors. Individual rainfall events are all captured and some noisy values are observed at the end of summer. In general, AMSR-E is very well capable of capturing the soil moisture dynamics.

The SMOS soil moisture retrievals capture the long-term dynamics while short-term dynamics are quite poorly captured. Observations are somewhat noisy and scarce, especially in the beginning of the

Table 3
Summary statistics of evaluation of three microwave satellites over Spain. The correlation (R, Eq. A.3), satellite standard error ($\dot{\sigma}_{\epsilon_s}$, Eq. 15) and bias ($\text{bias}_s$, Eq. 12) are calculated between the satellite soil moisture product and SWAP modeled soil moisture.

Number evaluated DGGs (−)	AMSR-E	SMOS	ASCAT
	438	440	680
Correlation (−)	0.682	0.420	0.713
Satellite standard error ($m^3\ m^{-3}$)	0.049	0.057	0.051
Bias ($m^3\ m^{-3}$)	0.018	−0.014	−0.019

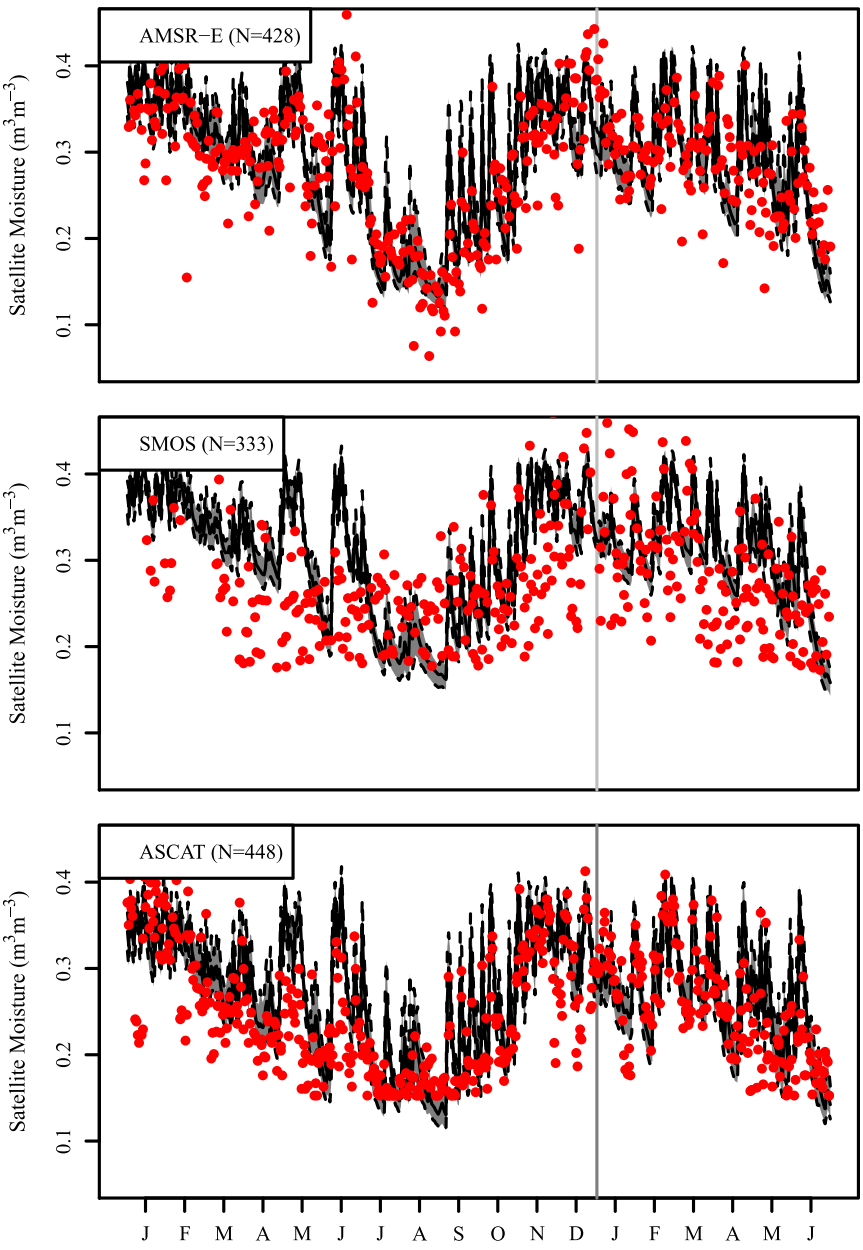

Fig. 7. Three example time series for AMSR-E, SMOS and ASCAT (red dotes) compared with the satellite support averaged SWAP soil moisture (black line), including 95% confidence interval (grey), N is the number of satellite soil moisture retrievals for one location in North West Spain (42.9° N, 2.7° W).

evaluation period. Although a rigorous filtering is performed there might still be some RFI disturbances which are not correctly flagged or detected. Successful retrievals show an underestimation of the soil moisture content and some unexpected peaks are present. These peaks are probably caused by an inaccurate assumption about the constant penetration depth during or short after precipitation events. In the second half of the evaluation period the performance of SMOS increases and precipitation events are captured more accurately. Also the number of retrievals is increased with exception of the period February 2011 when SMOS encountered technical problems with one of the arms of the satellite.

ASCAT shows a good correspondence with the modeled data, except for some small deviations in dry periods. The soil moisture response to precipitation events is captured well, resulting in high correlations (Table 3). A general characteristic of ASCAT soil moisture at this location is the tendency to show some deviations in summer from soil moisture calculated by the SWAP model, when soil moisture conditions are drier. This could be the result of volume scattering at low soil moisture values (Dorigo et al., 2010).

The correlation (R, Eq. A.3) and satellite product standard error ($\hat{\sigma}\epsilon_s$, Eq. 15) were used for the evaluation of all 79 reference locations and results are given in Fig. 8 and Table 3. ASCAT and AMSR-E both have a high R with the SWAP model simulation at all the DGG locations, while the R of SMOS is considerably lower. The high R values found for ASCAT and AMSR-E can be explained by the capability of both satellites to represent the short term soil moisture dynamics (Fig. **7**). R values of 0.8 are exceeded for 12% and 17% of the DGG locations for respectively AMSR-E and ASCAT, while SMOS does not have R values above 0.8. The average $\hat{\sigma}\epsilon_s$ of both AMSR-E and ASCAT is slightly lower in comparison with SMOS. However, none of the satellites satisfies the 0.04 $m^3\ m^{-3}$ accuracy which is set as a target for newly launched soil moisture missions like SMOS

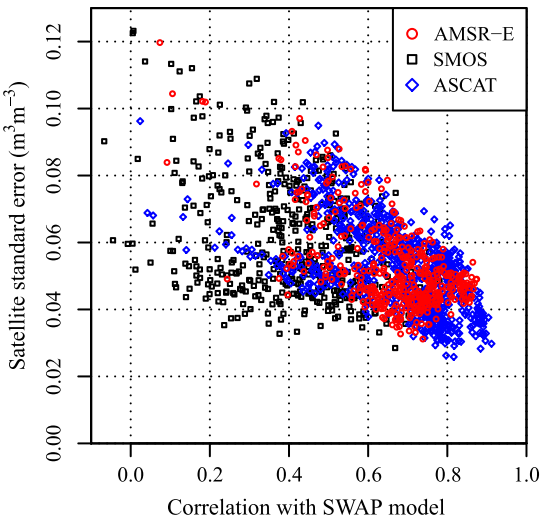

Fig. 8. Year-round correlation and satellite standard errors for all Digital Global Grid (DGG) satellite locations compared with SWAP model simulations for the period January 2010–June 2011 (one points is one DGG location).

(Kerr et al., 2001; Walker & Houser, 2004). ASCAT shows for 167 DGG locations a $\hat{\sigma}_{\epsilon_s}$ below 0.04 $m^3\ m^{-3}$, while for SMOS and AMSR-E satellite error values are only occasionally below this criterion (Fig. 8). A positive relation exists between the R and the $\hat{\sigma}_{\epsilon_s}$, in which a high R corresponds to a low $\hat{\sigma}_{\epsilon_s}$. After the transformation was applied (Eq. 1) a small negative $bias_s$ (Eq. 12) remains for SMOS and ASCAT (Table 3). Furthermore, although satellite soil moisture timeseries are given for specific DGG points, the spatial support may slightly change over time.

A spatial evaluation of the R and $\hat{\sigma}_{\epsilon_s}$ values for all satellite products is shown in Fig. 9. The correlation values are highest in the Southwestern part of Spain for all three satellite products and lowest in the North-Eastern locations for SMOS and ASCAT. AMSR-E shows low R values in the Northwest and high R values in the South and interior of Spain. Values for $\hat{\sigma}_{\epsilon_s}$ are lowest in Northern and central Spain with some high to very high values for AMSR-E and SMOS in the North-Western locations due to the proximity of the sea in combination with increased vegetation and topography. The spatial patterns of $\hat{\sigma}_{\epsilon_s}$ for both AMSR-E and ASCAT show a great resemblance to the patterns found with the triple collocation by Dorigo et al. (2010). The low R of ASCAT in the dry Eastern parts of Spain are most likely caused by the volume scattering effect in dry soils (Bartalis, Scipal & Wagner, 2006). Satellite products were compared and correlation between the different products as well as the anomalies were determined. The highest satellite correlations were found between AMSR-E and ASCAT ($R=0.536$), while correlations of SMOS with AMSR-E ($R=0.376$) and with ASCAT ($R=0.364$) are significantly lower. The correlation between AMSR-E and ASCAT is highest in the North-Western and Southern parts of Spain. These regions are also the areas where individual correlations with the SWAP model are highest for both satellites. The spatial patterns of the correlation between satellite products and correlations in ϵ_s are shown in Fig. C.15.

R values computed for ASCAT are higher than those found by Parrens et al. (2011) for France, while correlations found for SMOS are slightly lower. Correlations computed for AMSR-E are higher than in a recent inter-comparison study with observed in-situ data from Brocca et al. (2011) over Europe; the R values found for ASCAT are in the same range. An older study from Rüdiger et al. (2009) over France found similar R values as in this study for ASCAT. For AMSR-E, R values found in this study are higher, which is caused by the use of an improved version of the LPRM model. Comparison between in-situ data and both ASCAT and SMOS by Albergel et al. (2012) found lower R values for ASCAT and higher values for SMOS than obtained in this study.

In general, AMSR-E and ASCAT show the highest correlation for most DGG locations and capture the temporal soil moisture dynamics very well. The trend in the $\hat{\sigma}_{\epsilon_s}$ found in this study is similar to other

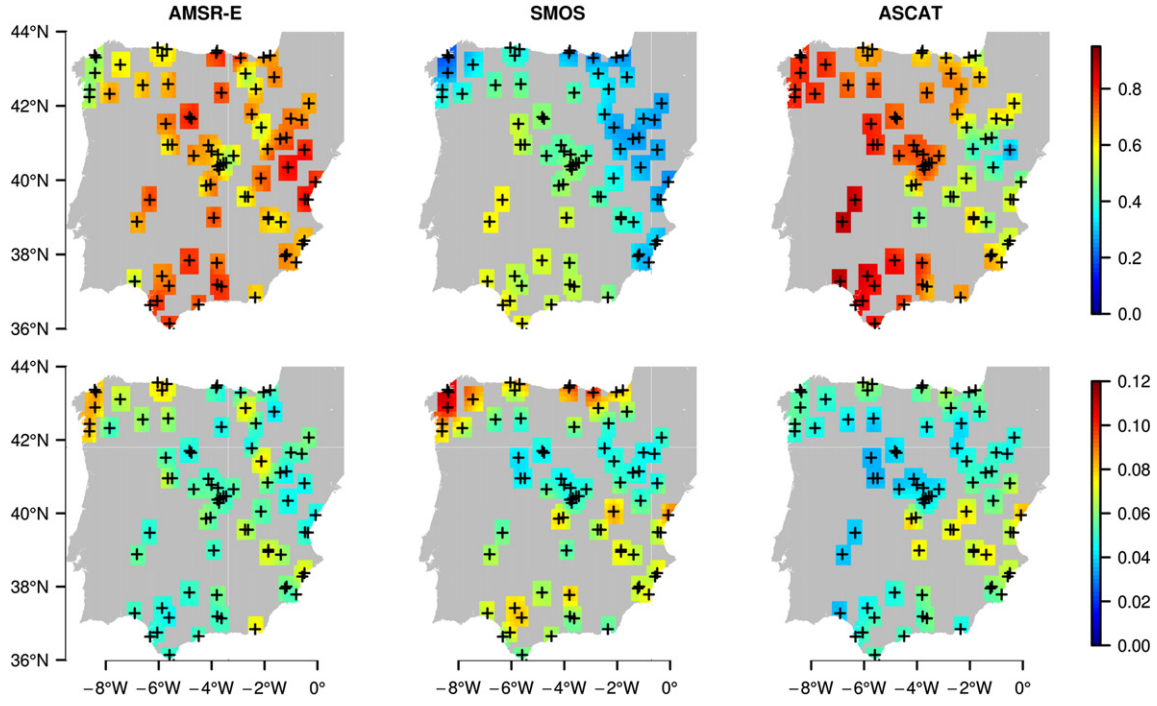

Fig. 9. Correlation, R, (top) and satellite standard error, $\hat{\sigma}_{\epsilon_s}$, (bottom) for the three satellite soil moisture products for the period January 2010–June 2011 over Spain. Meteorological stations are indicated by crosses.

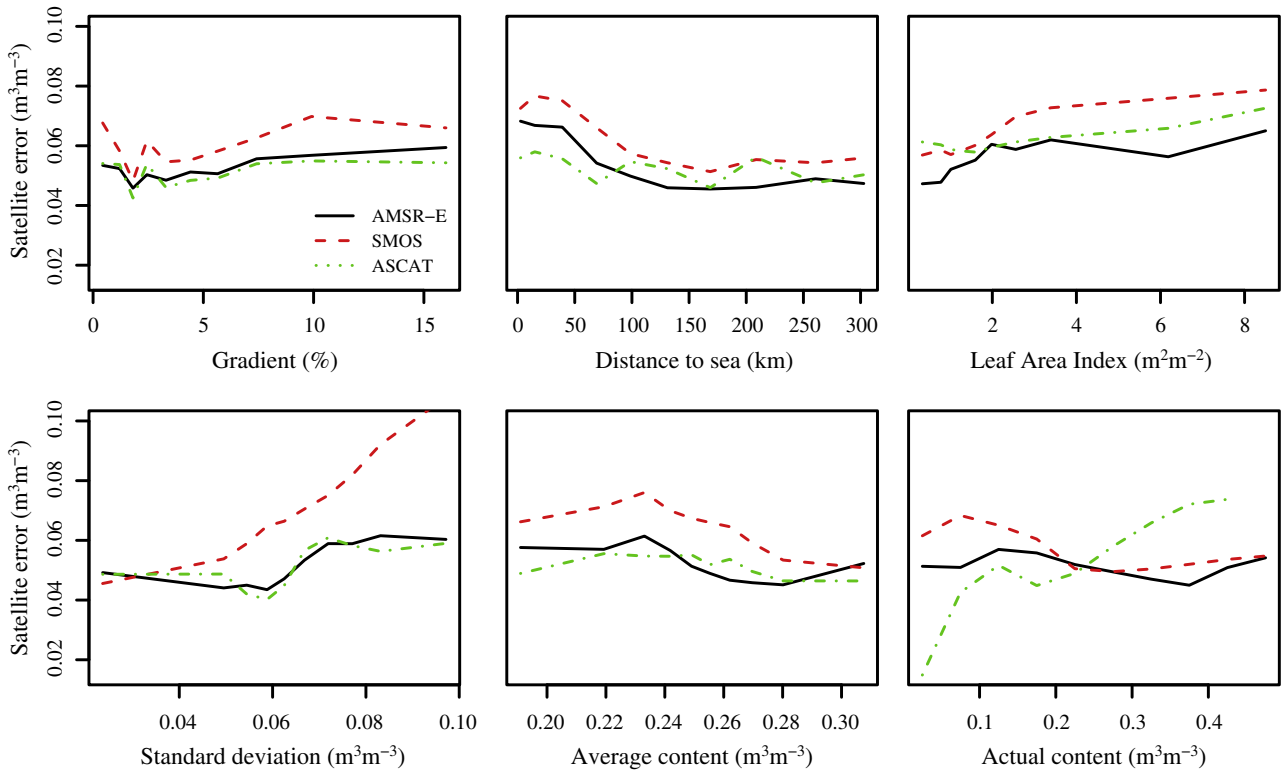

Fig. 10. Satellite standard error of satellite soil moisture for different factors in comparison with SWAP model for the period January 2010–June 2011 over Spain. The satellite error is $\hat{\sigma}_{\epsilon_s}$ (Eq. 15) is given for: the gradient (Grad), distance to the sea (Sea), standard deviation (σ_m) and μ_m. For the Leaf Area Index (LAI(t)) and actual content ($\theta(t)$) the bin-average time dependent satellite error is $_s(t)$ (Eq. 14) is shown.

studies (e.g. Albergel et al., 2012; Brocca et al., 2011; Parrens et al., 2011). However, a direct comparison is hampered by the fact that these studies did not incorporate model errors. Our approach accounts for model uncertainty and therefore gives a more correct estimation of the $\hat{\sigma}_{\epsilon_S}$ of satellite soil moisture products and the performance of space-born sensors.

3.3. Satellite error characterization

The effect of several external factors on the satellite standard error ($\hat{\sigma}_{\epsilon_S}$) is evaluated over Spain for all reference locations. The average slope of the location (Grad) is found to have negligible influence on the $\hat{\sigma}_{\epsilon_S}$ (Fig. 10), leading to the conclusion that gradients at the reference locations in Spain are too small to have a negative impact on $\hat{\sigma}_{\epsilon_S}$. However, with an increase in the distance to the sea (Sea), $\hat{\sigma}_{\epsilon_S}$ for AMSR-E and SMOS decrease. Above a distance of 100 to 150 km the influence of the sea is absent. An increase in the Leaf Area Index (LAI(t)) over time does influence the time dependent satellite error (ϵ_S, Eq. 14) in a negative way, ϵ_S increases with an increase in vegetation. The performance of SMOS is most affected by the average standard deviation of soil moisture (σ_m), where SMOS might have difficulties with highly dynamic soil moisture due to the high signal to noise ratio compared to AMSR-E and ASCAT. Over the entire modeling period (Jan 2010–Jun 2011), the average soil moisture content (μ_m) does not significantly influence the satellite performance, while the actual soil moisture content ($\theta(t)$) does have a large influence on the temporal performance of ASCAT. Both passive microwave satellites show a small increase in the ϵ_s for $\theta(t)$ between 0.1 and 0.2 $m^3\ m^{-3}$ and decrease thereafter. ASCAT shows an unambiguous increase in the ϵ_s with increasing $\theta(t)$. This could be the result of the strong response of ASCAT to precipitation events, while this response is less profound for AMSR-E and SMOS (Fig. 7). Correlations were most affected by changes in the average footprint soil moisture content (μ_m) and the distance to the sea (*Sea*) of all external factors understudy (not shown). In this study no strong relationship is found between the $\hat{\sigma}_{\epsilon_S}$ and the *Grad*. Based on previous studies (e.g. Engman & Chauhan, 1995) it was expected that the satellite performance was related to these properties. A relationship was found for *Sea*, *LAI*(t), σ_m, μ_m and $\theta(t)$ with $\hat{\sigma}_{\epsilon_S}$. This finding is confirmed by other studies (e.g. De Jeu et al., 2008; Njoku & Kong, 1977; Njoku & Li, 1999; Owe et al., 2008; Parinussa et al., 2011; Troch et al., 1996).

Finally, the error for all the remotely sensed soil moisture products is spatially correlated. Ranges of the variogram of correlation are between 100 and 220 km, for the three satellites products (Fig. 11). The correlation ranges, sill and nugget of the variogram are almost equal for all satellite products indicating that soil moisture errors have an almost identical spatial error pattern for AMSR-E, SMOS and ASCAT.

4. Conclusions

The soil moisture mapping accuracy of three satellite sensors was evaluated in this study. Satellites used in this study are passive microwave satellites AMSR-E and SMOS and the active microwave satellite ASCAT. Satellite soil moisture products were compared with the physically-based high resolution SWAP model. Soil moisture was modeled at a high vertical and horizontal resolution and averaged over the support of each satellite. A validation of the high-resolution SWAP model was performed on the REMEDHUS network situated in Spain. The mean modeled soil moisture from SWAP has a high correlation ($R = 0.878$) and low *RMSE* ($0.025 m^3 m^{-3}$) with the median of observations at the REMEDHUS site. From the predictive QQ-plot it was concluded that the SWAP model was able to capture the full probability density function in both space and time for this site. The

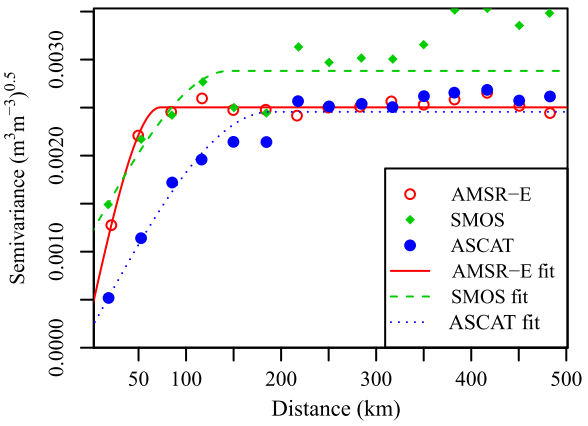

Fig. 11. Semi-variograms of the bin-average time dependent satellite product error ($_s(t)$) calculated for three satellite soil moisture products and the SWAP model, from all DGG locations for the period January 2010–June 2011 over Spain.

uncertainty added to meteorological input data as well as soil physical model parameters was enough to account for local variations in soil moisture values between observation points. From this validation at the REMEDHUS site it was concluded that the SWAP model can be used to simulate soil moisture with confidence over other areas of Spain.

The SWAP model was used to model the soil moisture content in Spain around 79 meteorological stations up to a distance of 35 *km* for the period January 2010 to June 2011. Satellite data was linearly transformed to match the dynamic range of the model to enable a valid comparison between satellite derived and modeled soil moisture. The AMSR-E data have a good correlation ($R=0.685$) with modeled SWAP soil moisture at the satellite support and the general yearly soil moisture trend is captured well. The short-term temporal dynamic and individual precipitation events are captured very well by AMSR-E, which results in a high correlation. SMOS shows a fair correlation with the SWAP model ($R=0.420$), the majority of precipitation events is captured, but in general soil moisture is underestimated compared to the model. However, it should be noted that the observation technique and algorithms of SMOS are still relatively new and improvements on the retrieval algorithm and flagging of RFI are constantly made leading to improved soil moisture retrievals. Of all products ASCAT showed the highest correlation with the SWAP model over Spain ($R=0.713$), which is mainly caused by the fact that precipitation events are captured very accurately. However, in summer the soil moisture values of ASCAT showed some noise. Correlations found in this study are in agreement with previous studies based on the comparison between satellite soil moisture and observational or modeled soil moisture data.

The error was expressed by using the satellite standard error ($\hat{\sigma}_{\epsilon_s}$), which also accounts for the model uncertainty. Therefore, $\hat{\sigma}_{\epsilon_s}$ is not overestimated as a result of a large model uncertainty. Average $\hat{\sigma}_{\epsilon_s}$ found were 0.049, 0.057, 0.051 m^3m^{-3} for AMSR-E, SMOS and ASCAT respectively, which is above the $\hat{\sigma}_{\epsilon_s}$ 0.04 m^3m^{-3}. Previous studies often lack a detailed assessment of the model uncertainty, resulting in an overestimation of $\hat{\sigma}_{\epsilon_s}$. In this study the model uncertainty was assessed in high detail, resulting in lower $\hat{\sigma}_{\epsilon_s}$ values and thus a lower satellite product error compared to other studies. From this comparison it is concluded that for an accurate estimation of $\hat{\sigma}_{\epsilon_s}$, a detailed assessment has to be made of the observation or model uncertainty in order not to overestimate the satellite product error. All three satellites have a bias ranging between -0.018 m^3 m^{-3} and 0.019 m^3 m^{-3} of which AMSR-E has the highest positive bias and ASCAT the lowest negative bias.

Additionally, a spatial comparison showed that all products show the highest correlation in the areas in the South West of Spain, which have a low average soil moisture content. The effects of land-sea contamination were found for AMSR-E and SMOS. Vegetation, soil moisture dynamics, average soil moisture content and the actual soil moisture content do have an impact on the satellite performance, where an increase of these factors negatively influences $\hat{\sigma}_{\epsilon_s}$. SMOS shows an increase in $\hat{\sigma}_{\epsilon_s}$ leading to the conclusion that SMOS has difficulties in accurately measuring soil moisture in highly dynamic soil moisture regimes. The performance of ASCAT was more correlated to actual soil moisture content, while there was no clear increase in $\hat{\sigma}_{\epsilon_s}$ for AMSR-E and SMOS. Semi-variogram models of the errors of all satellite soil moisture products for the entire simulation period show a spatial correlation in the error up to a distance of 150 km.

In general AMSR-E and ASCAT currently produce the best soil moisture time series. However, all three satellite products contain valuable information about the near-surface soil moisture over Spain.

Acknowledgments

This research was funded by a grant from the user support program Space Research of NWO (contract number NWO GO-AO/30). The authors would like to acknowledge Wouter Dorigo of the TU Wien, Jennifer Grant and Matthias Drusch at ESA-ESTEC, for their intellectual support on the topic of microwave remote sensing and especially on the topic of ASCAT and SMOS data. Both the Spanish meteorological service (AEMET) and the International Soil Moisture Network are acknowledged for making publicly available the meteorological and soil moisture data used in this study.

Appendix A. Equations

The Pearson correlation is given by:

$$R = \frac{\sum_{t=1}^{N}(\theta_o(t)-\mu_o)(\theta_m(t)-\mu_m)}{(N-1)\sigma_o\cdot\sigma_m} \tag{A.1}$$

where θ_o is the observed soil moisture (m^3m^{-3}), θ_m is the modeled soil moisture (m^3m^{-3}), μ_o is the average observed soil moisture over the entire simulation period (m^3m^{-3}), μ_m is the average modeled soil moisture over the entire simulation period (m^3m^{-3}), σ_o and σ_m are respectively the standard deviation of the observed and modeled soil moisture (m^3m^{-3}) and N is the total number of timesteps in the analysis. σ_o is calculated from the average observed soil moisture over the simulation period. The Root Mean Square Error (*RMSE*) is calculated as:

$$RMSE = \sqrt{\frac{\sum_{t=1}^{N}(\theta_m(t)-\theta_o(t))^2}{N}} \tag{A.2}$$

with N, the total number of observations. The correlation R for the evaluation of the remotely sensed soil moisture over Spain is calculated by:

$$R = \frac{\sum_{t=1}^{N}(\theta_m(t)-\mu_m)(\theta_s(t)-\mu_s)}{(N-1)\sigma_m\cdot\sigma_s} \tag{A.3}$$

where $\theta_s(t)$ is the satellite soil moisture (m^3m^{-3}), $\theta_m(t)$ is the modeled soil moisture (m^3m^{-3}), μ_s is the average satellite soil moisture over the entire simulation period (m^3m^{-3}), σ_m and σ_s are respectively the standard deviation of the modeled and satellite soil moisture (m^3m^{-3}) and N is the total number of timesteps in the analysis.

Appendix B. Example time series of selected locations

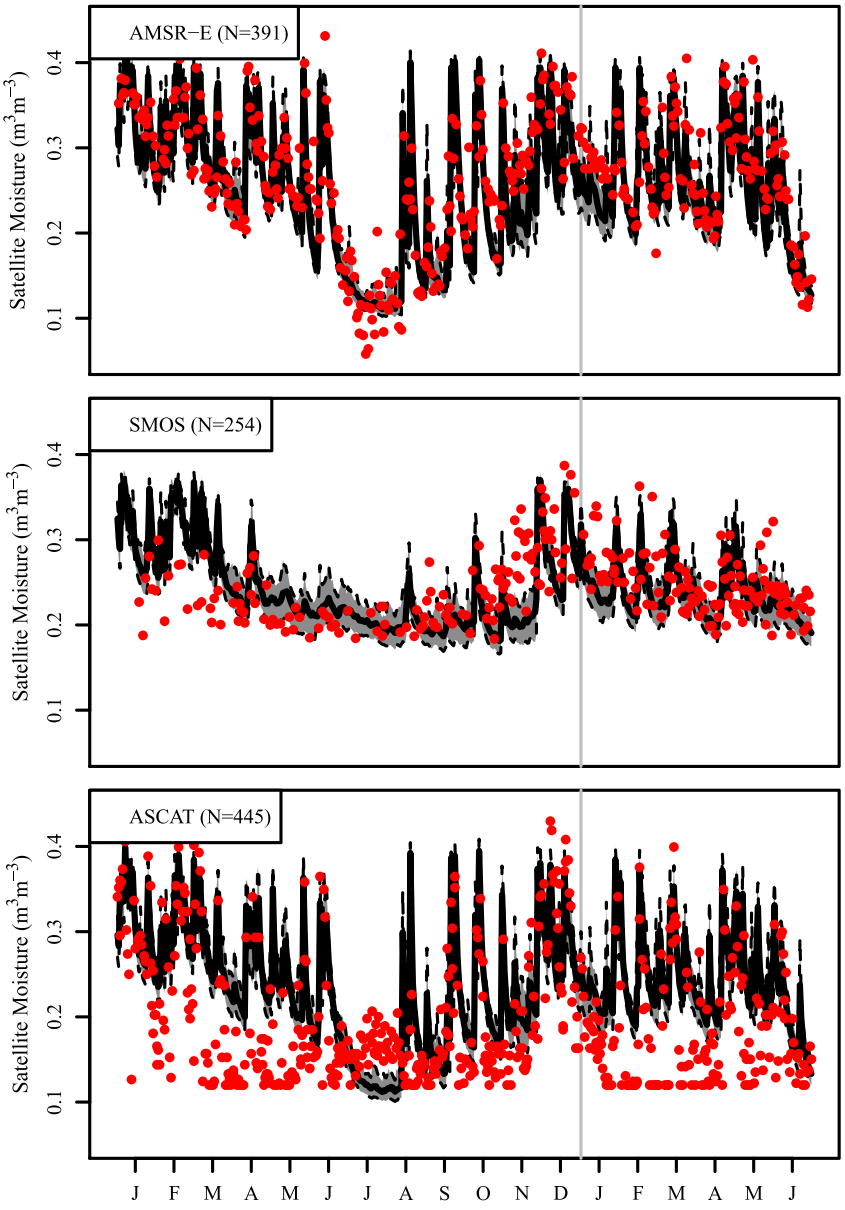

Fig. B.12 Three example time series for AMSR-E, SMOS and ASCAT compared with the satellite support averaged SWAP soil moisture (black line), including 95% confidence interval (grey), N is the number of satellite soil moisture retrievals for one location in South Spain (36.8° N, 2.4° W).

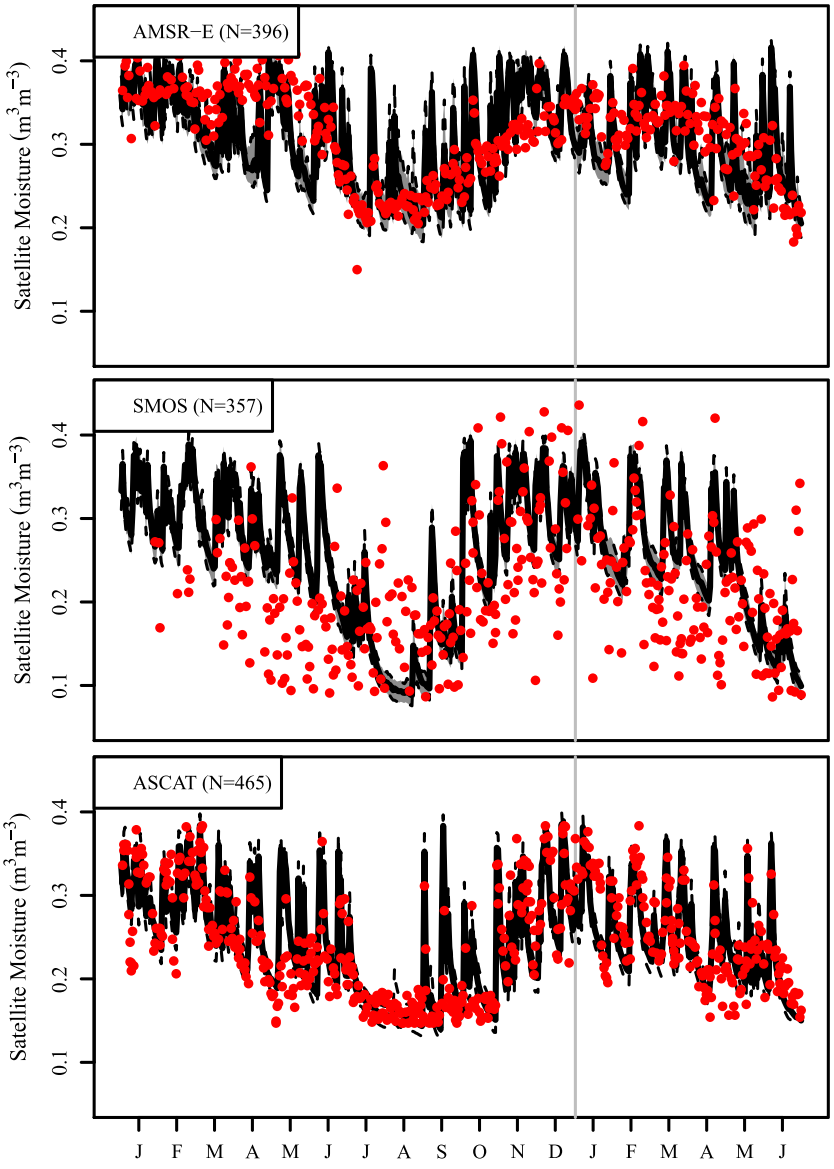

Fig. B.13. Three example time series for AMSR-E, SMOS and ASCAT compared with the satellite support averaged SWAP soil moisture (black line), including 95% confidence interval (grey), N is the number of satellite soil moisture retrievals for one location in Northeast Spain (42.8° N, 1.6° W).

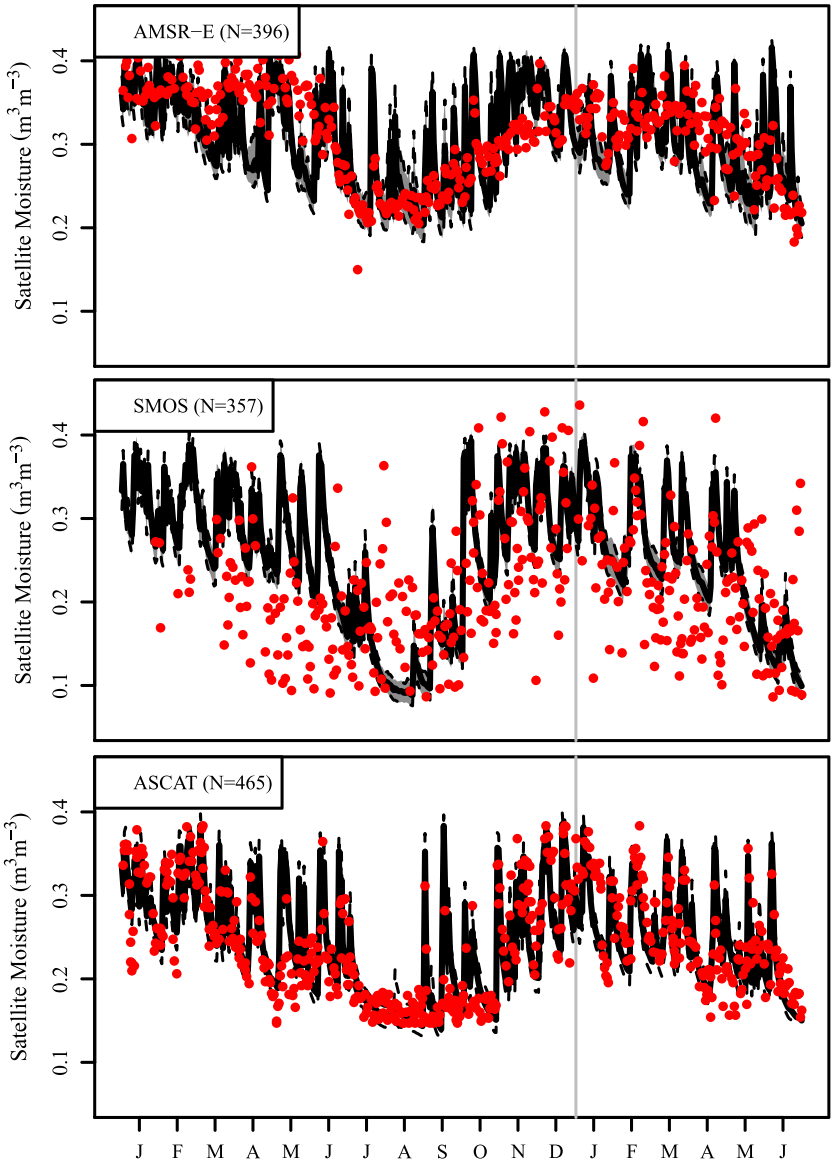

Fig. B.14. Three example time series for AMSR-E, SMOS and ASCAT compared with the satellite support averaged SWAP soil moisture (black line), including 95% confidence interval (grey), N is the number of satellite soil moisture retrievals for one location in central Spain (41.7° N, 4.8° W).

Appendix C. Spatial correlation between satellites

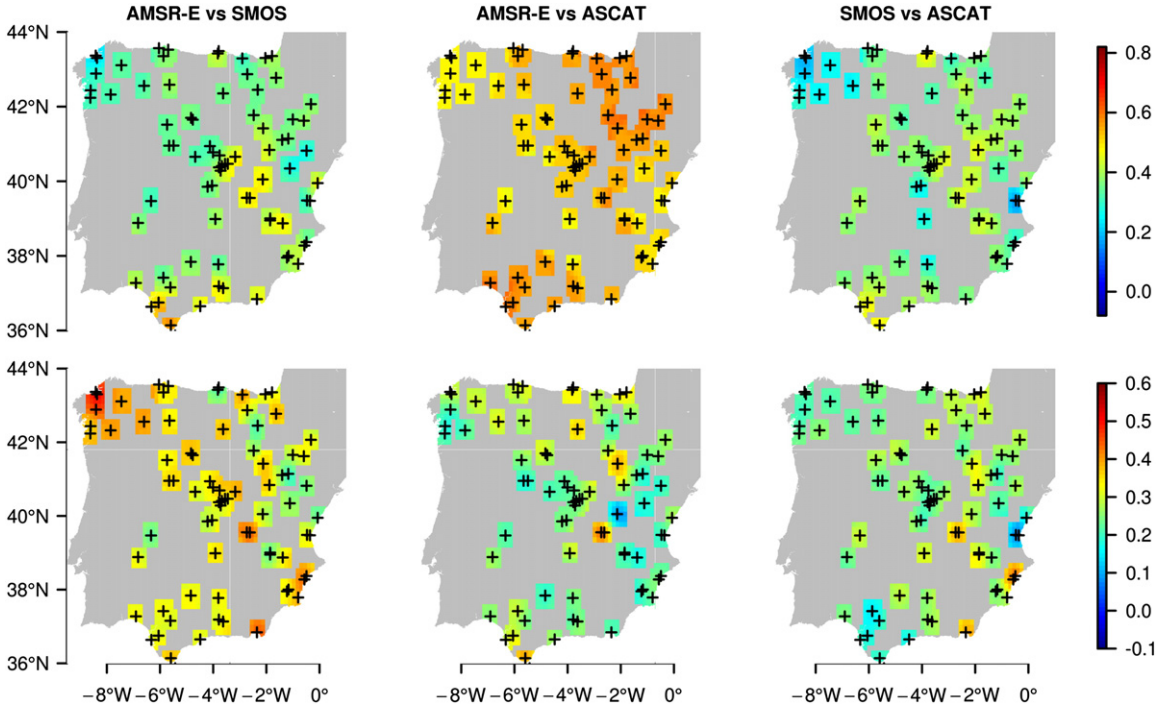

Fig. C.15. Correlation between satellite soil moisture products (top, R) and correlation between the satellite product errors (bottom, $_s(t)$) of different satellite products for the period January 2010–June 2011 over Spain, meteorological stations are indicated by crosses.

References

Albergel, C., Rosnay, P., Gruhier, C., Muñoz Sabater, J., Hasenauer, S., Isaksen, L., et al. (2012). Evaluation of remotely sensed and modelled soil moisture products using global ground-based in situ observations. *Remote Sensing of Environment*, *118*(15), 215–226.

Allen, R., Pereira, L., Raes, D., & Smith, M. (2006). FAO irrigation and drainage paper no. 56 — Crop evapotranspiration. Food and Agriculture Organization.

Anterrieu, E. (2011). On the detection and quantification of RFI in L1a signals provided by SMOS. *IEEE Transactions on Geoscience and Remote Sensing*, *49*(10), 3986–3992.

Baroni, G., Facchi, A., Gandolfi, C., Ortuani, B., Horeschi, D., & van Dam, J. C. (2010). Uncertainty in the determination of soil hydraulic parameters and its influence on the performance of two hydrological models of different complexity. *Hydrology and Earth System Sciences*, *14*(2), 251–270.

Bartalis, Z., Kidd, R., & Scipal, K. (2006). Development and implementation of a discrete global grid system for soil moisture retrieval using the metop ascat scatterometer. *1st EPS/MetOp RAO Workshop*. Frascati, Italy: ESA SP-618.

Bartalis, Z., Scipal, K., & Wagner, W. (2006). Azimuthal anisotropy of scatterometer measurements over land. *IEEE Geoscience and Remote Sensing Society*, *44*(8), 2083–2092.

Upscaling and downscaling methods for environmental research. Bierkens, M. F. P., Finke, P. A., & De Willigen, P. (Eds.). (2000). *Developments in Plant and Soil Sciences*, *Vol. 88*, : Kluwer Academic Publishers.

Bisselink, B., van Meijgaard, E., Dolman, A. J., & De Jeu, R. A. M. (2011). Initializing a regional climate model with satellite-derived soil moisture. *Journal of Geophysical Research*, *116*(D2), D02121.

Black, T. A., Gardner, W. R., & Thurtell, G. W. (1969). The prediction of evaporation, drainage, and soil water storage for a bare soil. *Soil Science Society of America Proceedings*, *33*(5), 655–660.

Brocca, L., Hasenauer, S., Lacava, T., Melone, F., Moramarco, T., Wagner, W., et al. (2011). Soil moisture estimation through ascat and amsr-e sensors: An intercomparison and validation study across europe. *Remote Sensing of Environment*, *115*(12), 3390–3408.

Brocca, L., Melone, F., Moramarco, T., Wagner, W., Naeimi, V., Bartalis, Z., et al. (2010). Improving runoff prediction through the assimilation of the ascat soil moisture product. *Hydrology and Earth System Sciences*, *14*(10), 1881–1893.

Cressie, N. A. C. (1993). *Statistics for spatial data.* Wiley series in Probability and mathematical statistics.

Crow, W. T., Berg, A. A., Cosh, M. H., Loew, A., Mohanty, B. P., Panciera, R., de Rosnay, P., Ryu, D., & Walker, J. P. (2012). Upscaling sparse ground-based soil moisture observations for the validation of coarse-resolution satellite soil moisture products. *Reviews of Geophysics*, *50*, RG2002. http://dx.doi.org/10.1029/2011RG000372.

Crow, W. T., Miralles, D. G., & Cosh, M. H. (2010). A quasi-global evaluation system for satellite-based surface soil moisture retrievals. *IEEE Transactions on Geoscience and Remote Sensing*, *48*(6), 2516–2527.

Crow, W. T., & Ryu, D. (2009). A new data assimilation approach for improving runoff prediction using remotely-sensed soil moisture retrievals. *Hydrology and Earth System Sciences*, *13*(1), 1–16.

Crow, W. T., & Zhan, X. (2007). Continental-scale evaluation of remotely sensed soil moisture products. *IEEE Geoscience and Remote Sensing Letters*, *4*, 451–455.

De Jeu, R. A. M., & Owe, M. (2003). Further validation of a new methodology for surface moisture and vegetation optical depth retrieval. *International Journal of Remote Sensing*, *24*, 4559–4578.

De Jeu, R. A. M., Wagner, W., Holmes, T. R. H., Dolman, A. J., Van de Giesen, N. C., & Friesen, J. (2008). Global soil moisture patterns observed by space borne microwave radiometers and scatterometers. *Surveys in Geophysics*, *28*, 399–420.

De Lannoy, G. J. M., Houser, P. R., Pauwels, V. R. N., & Verhoest, N. E. C. (2006). Assessment of model uncertainty for soil moisture through ensemble verification. *Journal of Geophysical Research*, *111*, D10101.

Dorigo, W. A., Scipal, K., Parinussa, R. M., Liu, Y. Y., Wagner, W., de Jeu, R. A. M., et al. (2010). Error characterisation of global active and passive microwave soil moisture datasets. *Hydrology and Earth System Sciences*, *14*(12), 2605–2616.

Dorigo, W. A., Wagner, W., Hohensinn, R., Hahn, S., Paulik, C., Xaver, A., et al. (2011). The international soil moisture network: A data hosting facility for global in situ soil moisture measurements. *Hydrology and Earth System Sciences*, *15*(5), 1675–1698.

Draper, C., Mahfouf, J. -F., Calvet, J. -C., Martin, E., & Wagner, W. (2011). Assimilation of ASCAT near-surface soil moisture into the sim hydrological model over France. *Hydrology and Earth System Sciences*, *15*(12), 3829–3841.

Draper, C., Walker, J. P., Steinle, P. J., De Jeu, R. A. M., & Holmes, T. R. H. (2009). An evaluation of amsr-e derived soil moisture over Australia. *Remote Sensing of Environment*, *113*, 703–710.

Drusch, M. (2007). Initializing numerical weather prediction models with satellite-derived surface soil moisture: Data assimilation experiments with ECMWF's integrated forecast system and the TMI soil moisture data set. *Journal of Geophysical Research*, *112*(D3), D03102.

Engman, E. T., & Chauhan, N. (1995). Status of microwave soil moisture measurements with remote sensing. *Remote Sensing of Environment*, *51*(1), 189–198.

Feddes, R. A., Kabat, P., Van Bakel, P. J. T., Bronswijk, J. J. B., & Halbertsma, J. (1988). Modelling soil water dynamics in the unsaturated zone — State of the art. *Journal of Hydrology*, *100*(1–3), 69–111.

Finke, P. A., Wösten, J. H. M., & Jansen, M. J. W. (1996). Effects of uncertainty in major input variables on simulated functional soil behaviour. *Hydrological Processes*, *10*(5), 661–669.

Harter, T., & Hopmans, J. (2004). Unsaturated-zone modeling: Progress, challenges, and applications. *Role of vadose-zone flow processes in regional-scale hydrology: review, opportunities and challenges* (pp. 179–208). Wageningen, The Netherlands, Ch.: Wageningen University.

Henderson-Sellers, A. (1996). Soil moisture: A critical focus for global change studies. *Global and Planetary Change*, *13*, 3–9.

Hengl, T., & Toomanian, N. (2006). Maps are not what they seem: representing uncertainty in soilproperty maps. In M. Caetano, & M. Painho (Eds.), *7th International Symposium on Spatial Accuracy Assessment in Natural Resources and Environmental Sciences*.

Kerr, Y., Pla, J., 2011. SMOS mission: description and radio frequency interference issue. retrieved on 01–02–2012. URL.

Kerr, Y. H., Waldteufel, P., Richaume, P., Wigneron, J. P., Ferrazzoli, P., Mahmoodi, A., Al Bitar, A., Cabot, F., Gruhier, C., Juglea, S. E., Leroux, D., Mialon, A., & Delwart, S. (2012, May). The SMOS soil moisture retrieval algorithm. *Geoscience and Remote Sensing, IEEE Transactions*, *50*(5), 1384–1403. http://dx.doi.org/10.1109/TGRS.2012.2184548

Kerr, Y., Waldteufel, P., Wigneron, J., Delwart, S., Cabot, F., Boutin, J., et al. (2010). The smos mission: New tool for monitoring key elements ofthe global water cycle. *Proceedings of the IEEE*, *98*(5), 666–687.

Kerr, Y., Waldteufel, P., Wigneron, J. -P., Martinuzzi, J., Font, J., & Berger, M. (2001). Soil moisture retrieval from space: The Soil Moisture and Ocean Salinity (SMOS) mission. *IEEE Transactions on Geoscience and Remote Sensing*, *39*(8), 1729–1735.

Kroes, J. G., van Dam, J. C., Groenendijk, P., Hendriks, R. F. A., & Jacobs, C. M. J. (2008). *SWAP version 3.2 — Theory description and user manual*. Wageningen: Alterra.

Laio, F., & Tamea, S. (2007). Verification tools for probabilistic forecasts of continuous hydrological variables. *Hydrology and Earth System Sciences*, *11*(4), 1267–1277.

Liu, Y. Y., Parinussa, R. M., Dorigo, W. A., De Jeu, R. A. M., Wagner, W., Van Dijk, A. I. J. M., et al. (2010). Developing an improved soil moisture dataset by blending passive and active microwave satellite-based retrievals. *Hydrology and Earth System Sciences Discussions*, *7*(5), 6699–6724.

Loew, A., Holmes, T. R. H., & De Jeu, R. A. M. (2009). The European heat wave 2003: Early indicators from multisensoral microwave remote sensing? *Journal of Geophysical Research*, *114*, D05103.

Martínez-Fernández, J., & Ceballos, A. (2003). Temporal stability of soil moisture in a large-field experiment in Spain. *Soil Science Society of America Journal*, *67*, 1647–1656.

Meesters, A. G. C. A., De Jeu, R. A. M., & Owe, M. (2005). Analytical derivation of the vegetation optical depth from the microwave polarization difference index. *IEEE Geoscience and Remote Sensing Letters*, *2*, 121–123.

Meyer, P. D., Rockhold, M. L., & Gee, G. W. (1997). Uncertainty analyses of infiltration and subsurface flow and transport for SDMP sites. *Tech. Rep. NUREG/CR-6565 PNNL-11705*. Washington: U.S. Nuclear Regulatory Commission Office of Nuclear Regulatory Research.

Miralles, D. G., Crow, W. T., & Cosh, M. H. (2010). Estimating spatial sampling errors in coarse-scale soil moisture estimates derived from point-scale observations. *Journal of Hydrometeorology*, *11*(6), 1423–1429.

Miralles, D. G., Holmes, T. R. H., De Jeu, R. A. M., Gash, J. H., Meesters, A. G. C. A., & Dolman, A. J. (2010). Global land-surface evaporation estimated from satellite-based observations. *Hydrology and Earth System Sciences Discussions*, *7*(5), 8479–8519.

Myneni, R., Knyazikhin, Y., Glassy, J., Votava, P., & Shabanov, N. (2003). *User's Guide FPAR, LAI (ESDT: MOD15A2) 8-day Composite NASA MODIS Land Algorithm*. NASA - Terra MODIS Land Team.

Naeimi, V., Scipal, K., Bartalis, Z., Hasenauer, S., & Wagner, W. (2009). An improved soil moisture retrieval algorithm for ERS and METOP scatterometer observations. *IEEE Transactions on Geoscience and Remote Sensing*, *47*(7), 1999–2013.

Njoku, E., Jackson, T. J., Lakshmi, V., Chan, T., & Nghiem, S. (2003). Soil moisture retrieval from AMSR-E. *IEEE Transactions on Geoscience and Remote Sensing*, *41*(2), 215–229.

Njoku, E. G., & Kong, J. A. (1977). Theory for passive microwave remote sensing of near-surface soil moisture. *Journal of Geophysical Research*, *82*(20), 3108–3118.

Njoku, E. G., & Li, L. (1999). Retrieval of land surface parameters using passive microwave measurements at 6-18 GHz. *IEEE Transactions on Geoscience and Remote Sensing*, *37*(1), 79–93.

Owe, M., De Jeu, R. A. M., & Holmes, T. R. H. (2008). Multisensor historical climatology of satellite-derived global land surface moisture. *Journal of Geophysical Research*, *113*, F01002.

Parinussa, R. M., Meesters, A. G. C. A., Liu, Y. Y., Dorigo, W. A., Wagner, W., & de Jeu, R. A. M. (2011). Error estimates for near-real-time satellite soil moisture as derived from the land parameter retrieval model. *IEEE Geoscience and Remote Sensing Letters*, *8*(4), 779–783.

Parrens, M., Zakharova, E., Lafont, S., Calvet, J. C., Kerr, Y., Wagner, W., et al. (2011). Comparing soil moisture retrievals from SMOS and ASCAT over France. *Hydrology and Earth System Sciences Discussions*, *8*(5), 8565–8607.

Richards, L. (1931). Capillary conduction of liquids through porous mediums. *Physics*, *1*, 318.

Rüdiger, C., Calvet, J. C., Gruhier, C., Holmes, T. R. H., De Jeu, R. A. M., & Wagner, W. (2009). An intercomparison of ERS-Scat and AMSR-E soil moisture observations with model simulations over France. *Journal of Hydrometeorology*, *10*(2), 431–447.

Sánchez, N., Martínez-Fernández, J., Calera, A., Torres, E., & Pérez-Gutiérrez, C. (2010). Combining remote sensing and in situ soil moisture data for the application and validation of a distributed water balance model (hidromore). *Agricultural Water Management*, *98*(1), 69–78.

Schuurmans, J. M., Bierkens, M. F. P., Pebesma, E. J., & Uijlenhoet, R. (2007). Automatic prediction of high-resolution daily rainfall fields for multiple extents: The potential of operational radar. *Journal of Hydrometeorology*, *8*, 1204–1224.

Scipal, K., Drusch, M., & Wagner, W. (2008). Assimilation of a ERS scatterometer derived soil moisture index in the ECMWF numerical weather prediction system. *Advances in Water Resources*, *31*(8), 1101–1112.

Sheffield, J., & Wood, F. (2007). Characteristics of global and regional drought, 1950–2000: Analysis of soil moisture data from off-line simulation of the terrestrial hydrologic cycle. *Journal of Geophysical Research*, *112*, D17115.

Siebert, S., Döll, P., Feick, S., Hoogeveen, J., Frenken, K., 2007. Global map of irrigation areas version 4.0.1. Map.

Singh, R., Kroes, J. G., van Dam, J. C., & Feddes, R. A. (2006). Distributed ecohydrological modelling to evaluate the performance of irrigation system in sirsa district, India: I. Current water management and its productivity. *Journal of Hydrology*, *329*(3–4), 692–713.

Troch, P. A., Vandersteene, F., Su, Z., Hoeben, R., & Wuethrich, M. (1996). Estimating microwave observation depth in bare soil through multi-frequency scatterometry. *Proceedings of the First EMSL User Workshop*. Ispra, Italy: SAI, JRC.

Van Dam, J. C., 2000. Field scale water flow and solute transport. SWAP model concepts, parameter estimation and case studies. Ph.D. thesis, Wageningen University.

Van Genuchten, M. T. (1980). A closed-form equation for predicting the hydraulic conductivity of unsaturated soils. *Soil Science Society of America Journal*, *44*, 892–898.

Van Leeuwen, P. J. (2009). Particle filtering in geophysical systems. *Monthly Weather Review*, *137*(12), 4089–4114.

Van Liedekerke, M., Jones, A., & Panagos, P. (2006). 1km raster version of the European soil database (v. 2.0). *Tech. Rep. EUR 19945 EN*. European Soil Bureau Network & European Commission.

Von Hoyningen-Hüne, J. (1983). Die interception des niederschlags in landwirtschaftlichen pflanzenbeständen. *Schriftenreihe des Deutschen Verbandes für Wasserwirtschaft und Kulturbau*, *57*, 17898.

Wagner, W., Blöschl, G., Pampaloni, P., Calvet, J. C., Bizzarri, B., Wigneron, J. P., et al. (2007). Operational readiness of microwave remote sensing of soil moisture for hydrologic applications. *Nordic Hydrology*, *30*(1), 1–20.

Wagner, W., Lemoine, G., & Rott, H. (1999). A method for estimating soil moisture from ERS scatterometer and soil data. *Remote Sensing of Environment*, *70*(2), 191–207.

Walker, J. P., & Houser, P. R. (2004). Requirements of a global near-surface soil moisture satellite mission: Accuracy, repeat time, and spatial resolution. *Advances in Water Resources*, *27*(8), 785–801.

Western, A. W., Grayson, R. B., & Bloschl, G. (2002). Scaling of soil moisture: A hydrologic perspective. *Annual Review of Earth and Planetary Sciences*, *30*, 149–180.

Wigneron, J. P., Chanzy, A., Calvet, J. C., & Bruguier, N. (1995). A simple algorithm to retrieve soil moisture and vegetation biomass using passive microwave measurements over crop fields. *Remote Sensing of Environment*, *51*(3), 331–341.

Yang, W., Tan, B., Huang, D., Rautiainen, M., Shabanov, N., Wang, Y., et al. (2006). Modis leaf area index products: From validation to algorithm improvement. *IEEE Transactions on Geoscience and Remote Sensing*, *44*(7), 1885–1898.